Calibration of phenological models for beech and oak tree species based on MODIS data

Roman Sitko, Peter Marčiš, Peter Valent, Ivan Barka, Marek Fabrika

Faculty of Forestry, Technical University in Zvolen

Summary

The comparison of three growing degree days GDD models for the prediction of spring phenology and calibration of one cooling degree days model for the prediction of autumnal phenological events are presented. Two Spring Warming models were used. The first one has a fixed beginning of the accumulation of forcing temperatures for the onset of spring phenological events. In the second model, the beginning of the accumulation is variable, depending on the daylength. Moreover, the parallel GDD model was tested, and in addition to forcing and daylength, the chilling accumulation was also considered. The process of leaf senescence and dormancy is modelled like an interaction of short daylength and low temperature in the autumn phenological model. All four models were calibrated on MODIS Land Cover Dynamics data with 500 m spatial resolution. The determination of the onset of phenological events such as i) Greenup, ii) Mid Greenup, iii) Maturity, iv) Peak, v) Senescence, vi) Mid Greendown, and vii) Dormancy is derived based on the 2-band Enhanced Vegetation Index EVI2 amplitude analysis. This MODIS product provides land surface phenology metrics at a yearly interval from 2001 to 2018. The mask of the forest stands with a dominant representation of beech and oak trees, within the territory of Slovakia was used. The time series of daily mean temperature for those stands were derived from E-OBS gridded observational dataset with a resolution of 0.1°. The statistics as RMSE, MAE, standard error and correlation coefficient were calculated with the aim to compare calibrated models. When comparing the GDD models, the day length proved to be an essential factor for improving the prediction of spring phenology. The higher accuracy achieved in the modelling of spring phenology compared to the autumn phenological events was confirmed.

Introduction

Spring and autumnal phenological events are closely linked to photosynthetic activities in temperate deciduous forests and consequently exerts a strong control on various ecological processes. Changes in spring leaf unfolding as well as in autumnal leaf senescence have significant implications for the length of the growing season (GARONNA et al. 2014), and hence for ecosystem production (KEENAN et al. 2014, PIAO et al. 2020). Therefore, the prediction of phenological events is an integral part of carbon cycle models at ecosystem and global scale (RICHARDSON et al. 2013).

The process-based phenological models are preferred in aim of simulating physiological processes and to yield more realistic predictions of growing season onset dates, contrary to empirical models. The timing of phenological events reflects a combination of internal settings (genetic) and environmental drivers (temperature, chilling, and photoperiod). The process-based models are grouped according to their scope of complexity to integrate the environmental drivers, into three categories (Basler, 2016):

1. models explaining ecodormancy release
2. models explaining the release of endo- and ecodormancy
3. models explaining the whole transition from dormancy induction until bud burst

The models explaining ecodormancy release are the oldest, accounting for thermal forcing in spring only and the degree days are used as forcing units. They use linear or sigmoid forcing function (HÄNNINEN 1990) to calculate the rate of forcing. The onset of the phenological event is identified at the moment of reaching the forcing requirements.

Currently more and more phenological models include the photoperiod as another explicit driver of spring and autumn phenology. MELAAS et al. (2016) observed that models for species more common in southern parts of the eastern part of US broadleaf forest tended to have lower photoperiod thresholds and higher forcing requirements, while models for more northern species tended to have higher photoperiod thresholds and lower forcing requirements. The spring phenology of the beech (*Fagus sylvatica*) was found to be controlled mainly by photoperiod for populations in southern and lower elevations and temperature for populations in northern and higher elevations (WAREING 1953). MENG et al. (2021) investigated that photoperiod-enabled models showed improvements in predicting spring leaf-out in terms of RMSE for six observed deciduous tree species and oak (*Quercus robur*) showed the most significant shift in the onset of leaf-out across latitude (1.7 days/°L). Also, for modeling of autumn phenophases of beech and oak is photoperiod key driver. DELPIERRE et al. (2009) notes, that photoperiod is triggering driver of senescence, although its progression is a result of cold temperatures.

The models explaining the release of endo- and ecodormancy are characterized by the inclusion of chilling requirements into spring phenological models as another driver of spring phenology. The chilling temperature (daily mean temperature between 0° - 5° C), indicating to the plant that winter has passed, plays an additional role in dormancy release of temperate and boreal trees. Chilling requirements are species-specific. Sessile oak (*Quercus petraea* (MATT) LIEBL.) has relatively low chilling requirements (90 days of chilling at < 5˚ C), although it has higher heat requirements compared to species such as beech (DANTEC et al. 2014) and contrary, beech is well-known by high chilling requirements. Fulfilling chilling requirements during the cold winter and spring leads to lower forcing requirements and thus to an earlier onset of spring phenological phases. Visa versa, failure to fulfil the chilling requirements of buds in dormancy period, during warm end of winter and spring, leads to an increase in the forcing requirements and thus also later bud burst (FADDEN 2019). Depending on the model's assumption regarding chilling and forcing interactions, Sequential, Parallel, Unified, Alternating, Dynamic etc. models are differentiated (BASLER 2016).

The models explaining the whole transition from dormancy induction until bud burst are the most sophisticated ones. The most complex models of this type integrate even the complex interactions of all three drivers of spring phenology, photoperiod with dormancy induction, chilling, and thermal forcing (CAFFARRA et al. 2011). However, no single model structure was found to predict spring phenology across different species, so the best predictive models are still species-specific (BASLER 2016).

A large and consistent dataset for model calibration is important to use, as using small sample size and inconsistent datasets of observations leads to reducing of the phenological models' accuracy for prediction of phenological events across different vegetation types and regions (WHITE et al. 1997). Satellites data can provide broad coverage of consistent information on vegetation phenology for diverse ecosystems at various scales and help to calibrate the phenology models. The data of spectroradiometer MODIS are very frequent source for calibrating phenological models. For this purpose, various characteristics derived from spectral reflectance data have been used, such as vegetation indices (PEANO et al. 2019), FPAR and LAI (STÖCKLI et al. 2011). Among the MODIS products, however, there is also a Land Cover Dynamics product (MCD123Q2), which is specifically aimed at identifying seven phe-

nological phases during growing season. FU et al. (2014) use this product for comparison four phenological models. MELAAS et al. (2013) compared start-of-season metrics between FLUXNET eddy covariance flux measurements and the Green-up phase identified within the MCD12Q2 product. It was found that the mentioned satellite metric can explain 70 % of the start-of-season variability of FLUXNET metrics in the deciduous broadleaf forest (DBF) sites. Specifically, the onset of spring green-up from MODIS was strongly correlated with 5 % Gross Ecosystem Productivity ratio across DBF sites ($r = 0.84$; $p < 0.01$).

However, the exclusive use of satellite metrics is suitable for calibrating models at the level of land surface phenology, which applies to generalized types of vegetation, such as deciduous broadleaf forest, evergreen needleleaf forest, mixed forest, etc., and are therefore not suitable for species-specific phenological models. MELAAS et al. (2016) recommends using a multiscale modelling approach for the calibration of such models, which is based on using the advantages of different sources of calibration data. Phenology data from individual trees provide detailed information regarding the nature and magnitude of within-species variability in phenology, but these patterns are hard to generalize at regional and larger scales. Satellite data, on the other hand, provide spatially integrated measurements for the timing of leaf onset over landscapes that include mixtures of species, plant functional types, and land cover types (KLOSTERMAN et al. 2014). In situ observation networks and remote sensing data can be used to synergistically calibrate and assess regional parameterizations of phenological models (MELAAS et al. 2016).

The main objective of this study is the calibration of a species-specific phenological models for beech (*Fagus sylvatica*) and oak (*Quercus robur* and *Qercus petraea*) tree species to determine the spring and autumn phenological events. Satellite phenological metrics were used in combination with forest inventory data of Slovakia. The data set and the used calibration procedures are an open system that has the potential to be extended to the other countries in Europe and temperate zone respectively. Another aim is the selection of the best spring and autumn prognostic phenological model and its implementation to the process-based Sibyl Lex Eterna model, which is being developed at the Faculty of Forestry, Technical University in Zvolen.

Material

Study sites of phenological observations are located in central Europe (Figure 1). Locations with a dominant composition of beech (*Fagus sylvatica*) and oak (*Quercus robur* and *Quercus petraea*) tree species were selected. Their latitudinal gradient of observation sites is around 1°N, longitudinal gradient is larger than 5°E, and altitudinal gradients are 984 m for beech localities and for oak localities 617 m respectively (Table 1). Long-term annual mean temperature calculated for period 1990-2019 ranges between 7.5-11.1°C on oak sites and 6.0-10.9°C on beech sites.

Table 1: Latitudinal, longitudinal, and altitudinal gradient of phenological observation sites

Tree specie	Latitude (°N)	Longitude (°E)	Altitude (m a.s.l.)
Beech	48.21-49.41	17.08-22.53	262-1246
Oak	47.95-48.97	17.04-22.28	159-776

The phenological observations are based on the analysis of the seasonal dynamics of the 2-band Enhanced Vegetation Index (EVI2), produced by the MODIS spectroradiometer, carried on the Terra and

Aqua satellites. The start of greenup (PP1-Greenup), greenup midpoint (PP2-MidGreenup), and maturity (PP3-Maturity) dates are retrieved as the first date within the greenup segment where the EVI2 time series crosses 15, 50, and 90 % of the greenup segment EVI2 amplitude (Figure 2). Similarly, start of senescence (PP5-Senescence), senescence midpoint (PP6-MidGreendown), and dormancy (PP7-Dormancy) are retrieved as the last date within the greendown segment where the EVI2 time series crosses 90, 50, and 15 % of the greendown segment EVI2 amplitude (GRAY et al. 2019). Phenological event named Peak is identified for the period of the growing season when EVI2 reaches its maximum. Those data are a component of MODIS Land Cover Dynamics product (MCD12Q2), created for period 2001-2018. Spatial resolution of the product is 500 m.

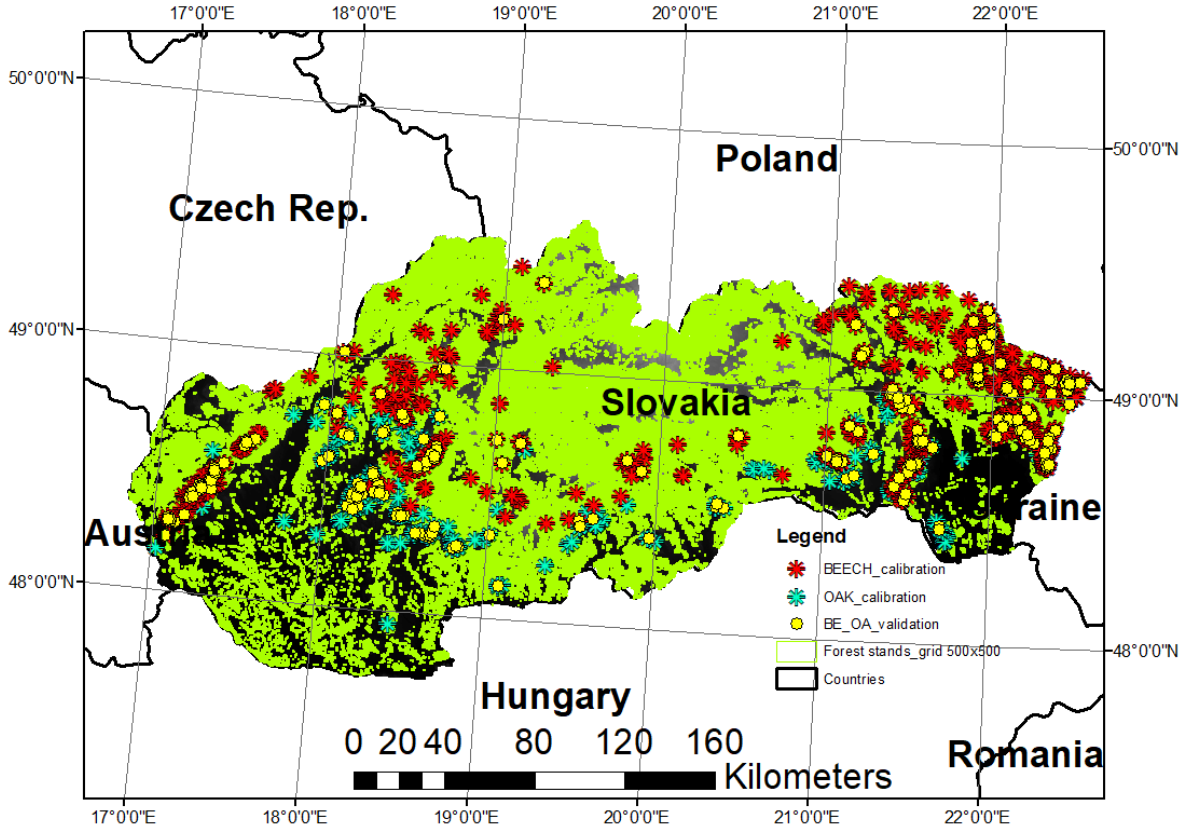

Figure 1: Sample design of phenological observations for OAK and BEECH forest stands

In order to calibrate the species-specific phenological model, data from the database of forest stands were used to identify locations with a dominant presence of beech or oak tree species. The territory of Slovakia was overlaid by a grid with the same distribution as the MCD12Q2 product. Those grid cells that met the following criteria were selected:

- 100 % of forest cover
- minimum 80 % or larger composition of oak or beech tree species
- stocking 0.7 or larger

A total of 1044 sites (18792 site-year observations) were selected, of which 773 were dominated by beech and 271 were dominated by oak. Approximately 75 % of the observations was used for calibration, and 25 % for validation of the models. By analyzing the interannual variability of NDVI within individual sites, locations with high variability were excluded from the selection. These may represent sites with a potential occurrence of disturbance events in the forest and were therefore excluded from the calibration process. Observations at the remaining locations were further subjected to the exclusion of observations with the occurrence of outliers.

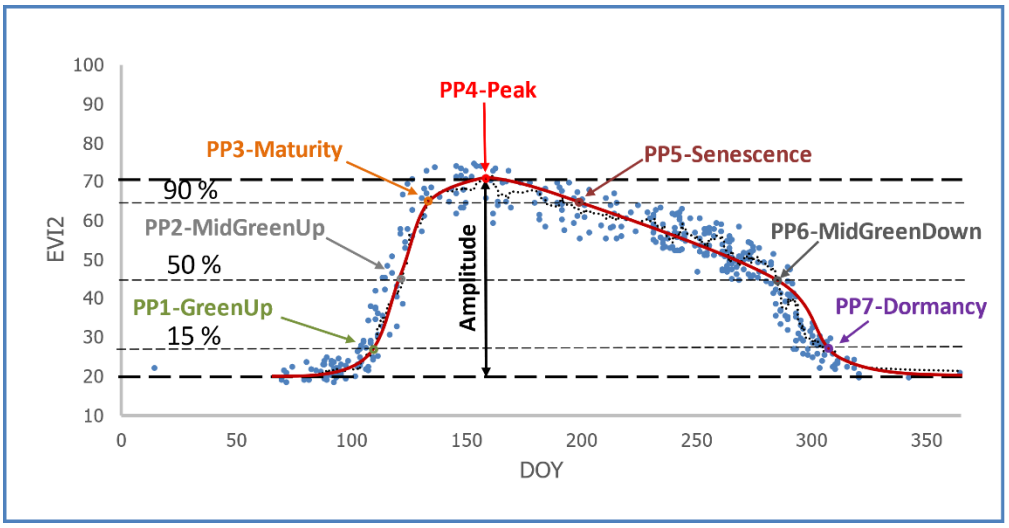

Figure 2: Phenological events determined by EVI2 amplitude analysis within the MODIS Land Cover Dynamics product

The time series of climatological data for the study sites during the period 2001–2018 was derived from the E-OBS gridded observational dataset version 25.0 at a 0.1° of Latitude and Longitude spatial resolution (CORNES et al. 2018).

Methods

Numerous models have been developed to simulate the events of spring phenology, such as bud burst or leaf unfolding, whereas only few models attempted to simulate the autumnal phases of phenology, such as leaf colouration and leaf fall (DELPIERRE et al. 2009). Efforts to understand the mechanisms and major drivers of leaf phenology have been largely placed on leaf unfolding, while for leaf senescence, relevant studies are fewer (LIU et al. 2020). We tested three models for predicting spring phenological events and one model for autumnal phenology. Spring phenological models were used to determine the onset of four phenological phases, Greenup, MidGreenup, Maturity and Peak (PP1-PP4). With the autumn model, we determined the onset of the MidGreendown and Dormancy phases (PP6-PP7). Senescence (PP5) was not predicted, due to the insufficiency of the selected models. The average onset of this phenological phase was found in the observations for beech on the 120th day of the year (DOY) and oak on the DOY 115. These days are part of the summer season; therefore, the use of spring and autumn models is not satisfactory.

Spring phenological models:

- Warming (MODEL 1)
- Photo-threshold (MODEL 2)
- Photo-chilling (MODEL 3)

Autumn phenological model:

- Cooling-shortening (MODEL 4)

MODEL 1 - Spring warming model

The model is based on accumulation of thermal forcing to evaluate state of forcing (Sf) as a sum of rate of forcing (R_f) (2), and Rf is computed as a function of air temperature using a logistic function (1) SARVAS (1974):

$$R_f = \begin{cases} \dfrac{28.4}{1 + \exp(3.4 - 0.185 * x)} & x > 0 \\ 0 & x \leq 0 \end{cases} \qquad \textit{Eq. 1}$$

$$S_f(t) = \sum_{t_0}^{t} R_f(x) \qquad \textit{Eq. 2}$$

where *x* is daily mean air temperature, t_0 is the start DOY when forcing begins to accumulate (set up to the 1st of January for the warming model), and *t* is the DOY for the onset of a phenological event, which occurs when S_f reaches a prescribed threshold $S_f(t) \geq F^*$. F^* threshold value is parametrized as linear function of long-term mean annual temperature $F^* = f(T_{1990-2019})$ calculated for period 1990-2019 and $T_{1990-2019}$ is a linear function of longitude, latitude and altitude $T_{1990-2019} = f(Lon, Lat, Alt)$ in our research. MELAAS et al. (2013) used this approach to account for variability in climatology related to geographic patterns, because thermal forcing required for spring onset is lower at more northern sites than at southern sites in the Northern Hemisphere.

MODEL 2 - Spring photo-threshold model

Photo-treshold model reflects the knowledge, that daily daylength exceeding some threshold can compensate lack of forcing for onset of phenological events. It is used the same approach to evaluate Sf as it is in warming model (2) except two differences related to comprising daily daylength (*DL*) as another variable for prediction of spring phenology. The forcing process starts at t_0, that is flexible DOY when $DL \geq DL_{start}$, where DL_{start} is the minimum daily daylength threshold to trigger the forcing process. The second difference is that spring phenology is predicted to occur not only when forcing accumulation reaches its threshold ($S_f(t) \geq F^*$) but also when daylength *DL* is above a maximum threshold DL ≥ DLend (MELAAS et al. 2016). Parameters DL_{start}, DL_{end},for beech and oak tree species were taken from MENG et al. (2021). Daylength was calculated as a function of latitude (L) and day of the year (DOY) using Equation (FABRIKA u. PRETZSCH 2013).

MODEL 3 - Spring photo-chilling model

The model considers all three main drivers of spring phenology: temperature, chilling, and photoperiod. The photo-chilling model was developed from a widely used chilling model, that is, parallel model, which considers the forcing and chilling processes (HÄNNINEN 1990), and moreover, a chilling-dependent photoperiod variable Rp to this model was added to adjust the efficiency of forcing accumulation (MENG et al. 2021).

$$R_f = \begin{cases} \dfrac{28.4}{1 + \exp(3.4 - 0.185 * x)} & x > T_{base} \\ 0 & x \leq T_{base} \end{cases} \qquad \textit{Eq. 3}$$

$$R_c = \begin{cases} 0 & x \geq 10.4 \; or \; x \leq -3.4 \\ \dfrac{x + 3.4}{T_{opt} + 3.4} & -3.4 < x \leq T_{opt} \\ \dfrac{x - 10.4}{T_{opt} - 10.4} & T_{opt} < x < 10.4 \end{cases} \qquad \textit{Eq. 4}$$

$$R_p = \frac{DL}{12} * e^{c * R_c} \qquad \textit{Eq. 5}$$

$$S_f(t) = \sum_{t_0}^{t} \left(R_f(x) * R_P(DL, R_c)\right) \quad \textit{Eq. 6}$$

$$S_c(t) = \sum_{t_0}^{t} R_c(x) \quad \textit{Eq. 7}$$

Spring events are predicted to occur when $S_f(t) \geq a.e^{b*S_c(t)}$, where $b < 0$; t is the DOY for onset of phenological event, x is daily mean temperature, DL is daily daylength, T_{opt} is the optimum temperature for chilling accumulation, $Sf(t)$ and $Sc(t)$ are the state of forcing and chilling respectively; R_f (3), R_c (4), and R_p (5) are the rate of forcing, chilling, and photoperiod respectively. Forcing and chilling accumulation starts at t_0, that is set up to the 1st of November in the preceding year in this study; T_{base} is base temperature (5°C); a, b, c, and T_{opt} are parameters to be calibrated.

MODEL 4 - Autumn cooling-shortening model

The process of leaf senescence (i. e., dormancy induction) is co-triggered by a function of short daylength DR_P and a function of low temperatures DR_T, and is completed when the state of dormancy induction DS (8) reaches a critical value $DS(t) \geq D_{crit}$ (LIU et al. 2020):

$$DS(t) = \sum_{t_0}^{t} (DR_T * DR_P) = \sum_{t_0}^{t} \left(\frac{1}{1 + e^{aD*(x-bD)}} \times \frac{1}{1 + e^{cD*(DL-DL_{crit})}}\right) \quad \textit{Eq. 8}$$

where t_0 is the start date of dormancy induction (fixed to the 1st of September of the current year), and t is the DOY for the onset of a phenological event; x is daily mean air temperature and DL is daily daylength; DL_{crit}, aD,bD and cD are specie-specific function parameters taken from LIU et al. (2020) derived for two kinds of phenological observations – i) ground-based, ii)satellite-based; and D_{crit} was calibrated on calibration sample of MCD12Q2 observations, in case of using the function parameters derived from satellite-based observations (LIU et al. 2020), $D_{crit}=f(Altitude)$ for beech and $D_{crit}=f(T_{1990\text{-}2019})$ for oak in our study, otherwise D_{crit} was calibrated as average of $DS(t)$ of calibrating sample.

Root Mean Square Error (RMSE), Mean Absolute Error (MAE) and Standard Error (SE) were used to indicate the discrepancies between observed and predicted onsets of phenological events. RMSE indicates overall accuracy of the predictions. MAE indicates bias of the model, and p-value was calculated to evaluate significance of bias. SE indicates the precision of the predictions. The relation between the errors describes equation (9). Correlation between observations and predictions was measured by correlation coefficient (R).

$$RMSE = \sqrt{MAE^2 + SE^2} \quad \textit{Eq. 9}$$

Results

The first part of results is focused on individual evaluation and mutual comparison of the models for prediction of onset of spring phenological phases (PP1-PP4) and autumn phenological phases (PP6-PP7).

Spring warming model brings better predictions of phenological events for oak compared to beech. Correlation coefficients range between 0.34-0.79 for spring phenology of oak. The highest were correlated predictions with observations of PP2-MidGreendown, the lowest correlation was found out for

PP4-Peak (Table 2). Similar proportion between phenological phases was observed in modeling of beech spring phenology, while correlation coefficients are in interval 0.25-0.41. Also, the accuracy of the warming model was higher for oak than for beech. Within the phenological phases, the difference between tree species RMSE was from ±2.68 days for PP4 to ±3.76 days for PP2. Accuracy for spring phenological models of beech ranges from ±8.19 (PP2) – ±11.18 days (PP1), for oak from ±4.43 (PP2) – ±8.20 days (PP1-Greenup) (Table 2).

The introduction of daylength into the spring photoperiod-threshold model resulted to the significant increase in correlations for beech and, conversely, a slight decrease of correlation coefficients for oak spring phenological phases. Exception was PP4, where R increased for both tree species comparing to warming model (Table 2). The accuracy of the model also increased in all phenological phases for beech, most significantly in PP1, where RMSE decreased to ±8.32 days, which is still the lowest accuracy of this model for beech spring phenology. The highest accuracy was found for PP2, RMSE=±6.53 days. Accuracy of modeling of oak spring phenology increased in PP1 and PP4 (the highest RMSE=±7.68 days of the model for oak), and slightly decreased in PP2 (the lowest RMSE=±4.6 days of the model for oak) and PP3-Maturity (Table 2).

The different use of the daylength in the spring photo-chilling model, comparing to the photo-threshold model, brought an increase in the correlation for all phenological phases and tree species, only at PP4 the R remained at an unchanged value of 0.37 (Table 2) for oak. Predicted and observed onsets are most closely correlated for both tree species in PP2 (R=0.60 and 0.78 respectively), the least closely in PP1 for beech (R=0.40) and in PP4 for oak (R=0.37). Accuracy of the model has stayed almost at the same level as it is in photo-threshold model, just at PP1 decreased more significant for beech (RMSE=±9.94 days), less significant for oak (RMSE=±7.14 days) (Table 2).

Autumn cooling-shortening model was calibrated for two sets of parameters of Equation (8), i) ground-based and ii) satellite-based LIU et al. (2020). From the point of view of the power of correlation between the predicted onset of the autumn phenological phases (PP6-MidGreendown and PP7-Dormancy) and the observed one within the MODIS product MCD12Q2, the parameters derived from ground-based observations according to Liu et al. (2020) proved to be more appropriate. Correlation coefficients of the model acquired higher values for both phenological phases and tree species using these parameters, except the phase PP7 for beech (Table 3). Parameters derived using satellite-based phenological observations (LIU et al. 2020) endorsed the autumn model for predicting the Dormancy of beech tree species compared to "*ground-based*" parameters. Correlation coefficient increased from 0.19 to 0.34. Correlation for both phases was higher for beech in comparison with oak. On the contrary, the accuracy of autumn phenology modeling for PP6 and PP7 was higher for oak (RMSE=±4.66 and ±4.76 days), for beech RMSE was equal to ±6.65 days (PP6) and ±7.25 days (PP7) respectively (Table 3).

Table 2: Evaluation of spring phenological models for Greenup (PP1), MidGreenup (PP2), Maturity (PP3) and Peak (PP4) (root mean square error RMSE, mean absolute error MAE and standard error SE are measured in days; p-value indicate significance of MAE; R – correlation coefficient between predictions and observations; n – validation sample size)

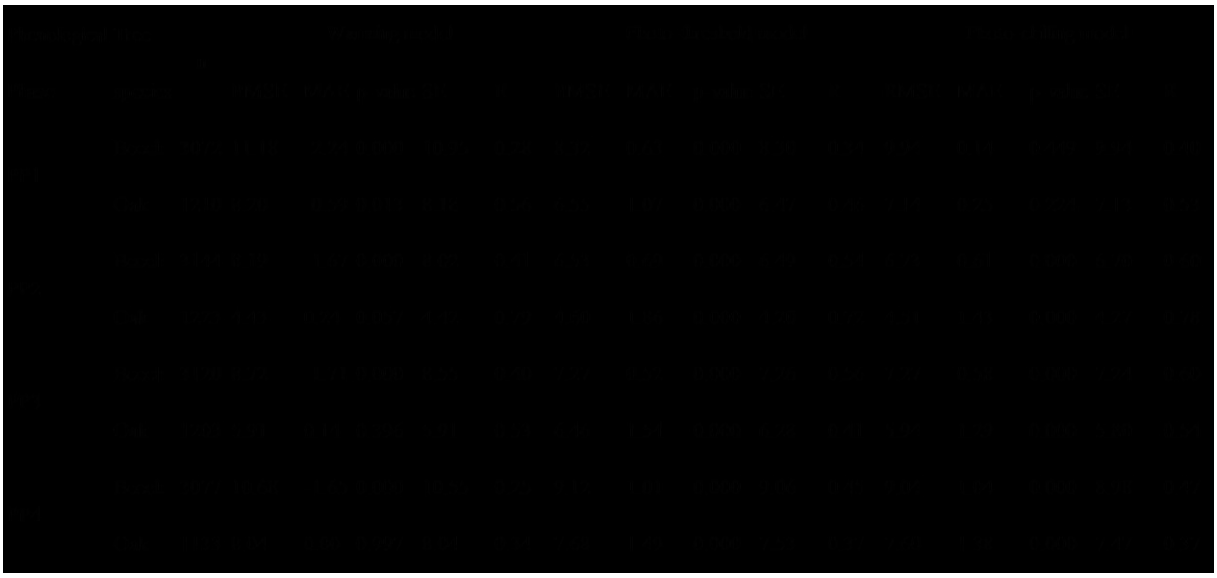

Table 3: Evaluation of autumn phenological model for MidGreendown (PP6), Dormancy (PP7) (Root Mean Square Error (RMSE), Mean Absolute Error (MAE) and Standard Error (SE) are measured in days; p-value indicate significance of MAE; R – correlation coefficient between predictions and observations; n – validation sample size; satellite-based – parameters used from parametrization of the model on satellite-based observations (LIU et al. 2020); ground-based – parameters used from parametrization of the model on ground-based observations (LIU et al. 2020)

Phenological Phase	Tree species	n	Cooling-shortening model (satellite-based parameters)					Cooling-shortening model (ground-based parameters)				
			RMSE	MAE	p-value	SE	R	RMSE	MAE	p-value	SE	R
PP6	Beech	3139	6.89	1.11	0.000	6.80	0.36	6.65	1.21	0.000	6.54	0.43
	Oak	1161	4.74	0.04	0.766	4.74	0.06	4.66	-0.02	0.890	4.66	0.26
PP7	Beech	3163	7.25	1.14	0.000	7.16	0.34	7.77	1.28	0.000	7.66	0.19
	Oak	1193	4.39	0.22	0.089	4.39	0.03	4.76	0.29	0.038	4.76	0.12

The different use of the daylength in the spring photo-chilling model, comparing to the photo-threshold model, brought an increase in the correlation for all phenological phases and tree species, only at PP4 the R remained at an unchanged value of 0.37 (Table 2) for oak. Predicted and observed onsets are most closely correlated for both tree species in PP2 (R=0.60 and 0.78 respectively), the least closely in PP1 for beech (R=0.40) and in PP4 for oak (R=0.37). Accuracy of the model has stayed almost at the same level as it is in photo-threshold model, just at PP1 decreased more significant for beech (RMSE=±9.94 days), less significant for oak (RMSE=±7.14 days) (Table 2).

Autumn cooling-shortening model was calibrated for two sets of parameters of Equation (8), i) ground-based and ii) satellite-based Liu et al. 2021. From the point of view of the power of correlation between the predicted onset of the autumn phenological phases (PP6-MidGreendown and PP7-Dormancy) and the observed one within the MODIS product MCD12Q2, the parameters derived from ground-based observations according to LIU et al. (2020) proved to be more appropriate. Correlation coefficients of the model acquired higher values for both phenological phases and tree species using these parameters, except the phase PP7 for beech (Table 3). Parameters derived using satellite-based phenological observations (LIU et al. 2020) endorsed the autumn model for predicting the Dormancy of beech tree species compared to "*ground-based*" parameters. Correlation coefficient increased from 0.19 to 0.34. Correlation for both phases was higher for beech in comparison with oak. On the contrary, the accuracy of autumn phenology modeling for PP6 and PP7 was higher for oak (RMSE=±4.66 and ±4.76 days), for beech RMSE was equal to ±6.65 days (PP6) and ±7.25 days (PP7) respectively (Table 3).

The best results for modeling the onset of the spring phenological phases of beech were found with the photo-chilling model (MODEL 3). In case of phenological phases where the p-value of mean average error MAE does not exceed significant level of 5 % (Table 2), bias was removed from the model by subtracting the value of MAE from the predicted DOY of onset of the phenological phase. In that case, the root mean square error RMSE coincides with the standard error SE value, what follows from Equation (9).

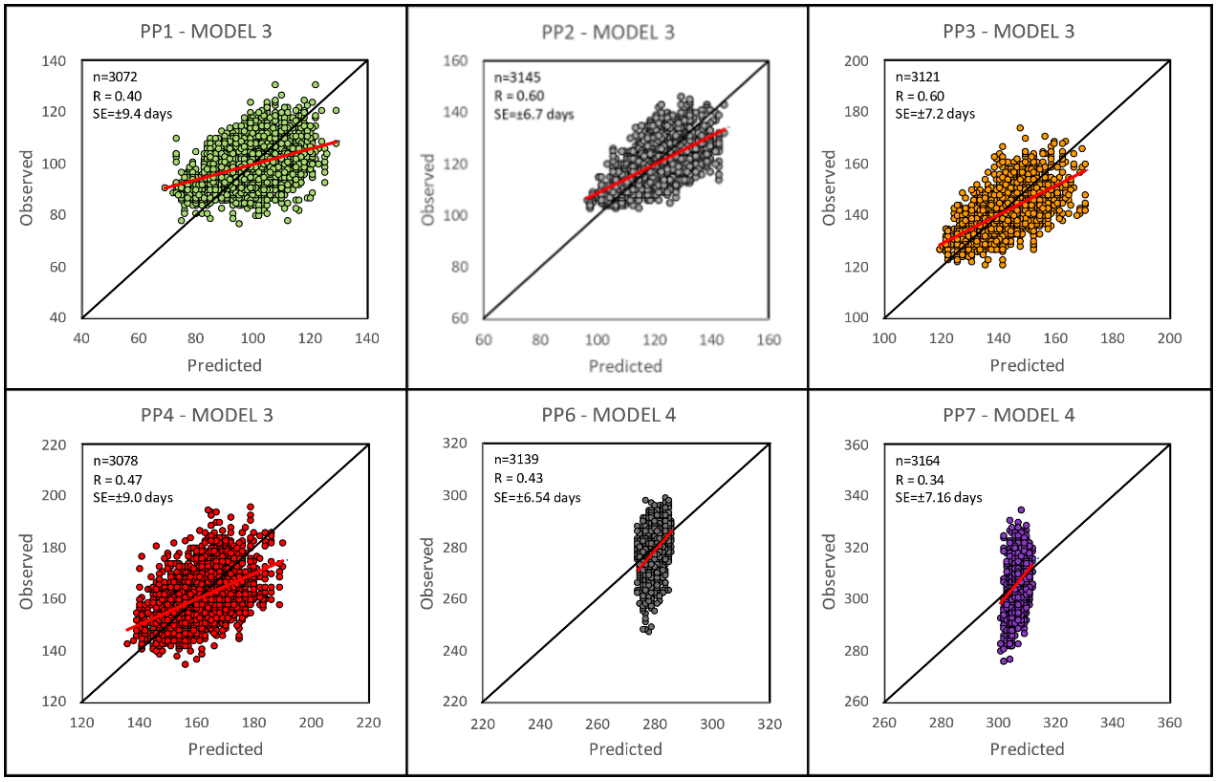

Figure 3: Statistics of the best choosen phenological models of beech for prediction of spring (PP1-PP4) and autumn (PP6-PP7) phenological phases (MODEL 3 – Spring photo-chilling, MODEL 4 – Autumn cooling-shortening)

Predictions of spring phenological phases (PP1-PP4) for beech were higher correlated with the observations when autumn predictions (Figure 3). The highest correlation was evaluated for PP2 and PP3 (R=0.60), the lowest for PP7 (R=0.34). Precision of predictions is in the range of ±6.54 days for PP6 to ±9.4 days for PP1 and this error should not be exceeded with 68 % probability. SE of prediction of the onset of autumn phenological phases (PP6-PP7) was ±6.54 days and ±7.16 days respectively (Figure 3).

For oak, MODEL 1 proved to be the best model for modeling phenological phases PP1, PP2, and MODEL 3 for phases PP3 and PP4. The precision of these models ranges from SE=±4.4 days for PP2 to SE=±8.2 days for PP1, and correlation coefficients from R=0.37 for PP4 to R=0.79 for PP2 (Figure 4). Predictions of the onset of autumn phases for oak were poorly correlated with observations, R=0.26 for PP6 and R=0.12 for PP7. The precision of these models is equal to SE=±4.7 days and ±4.8 days respectively (Figure 4).

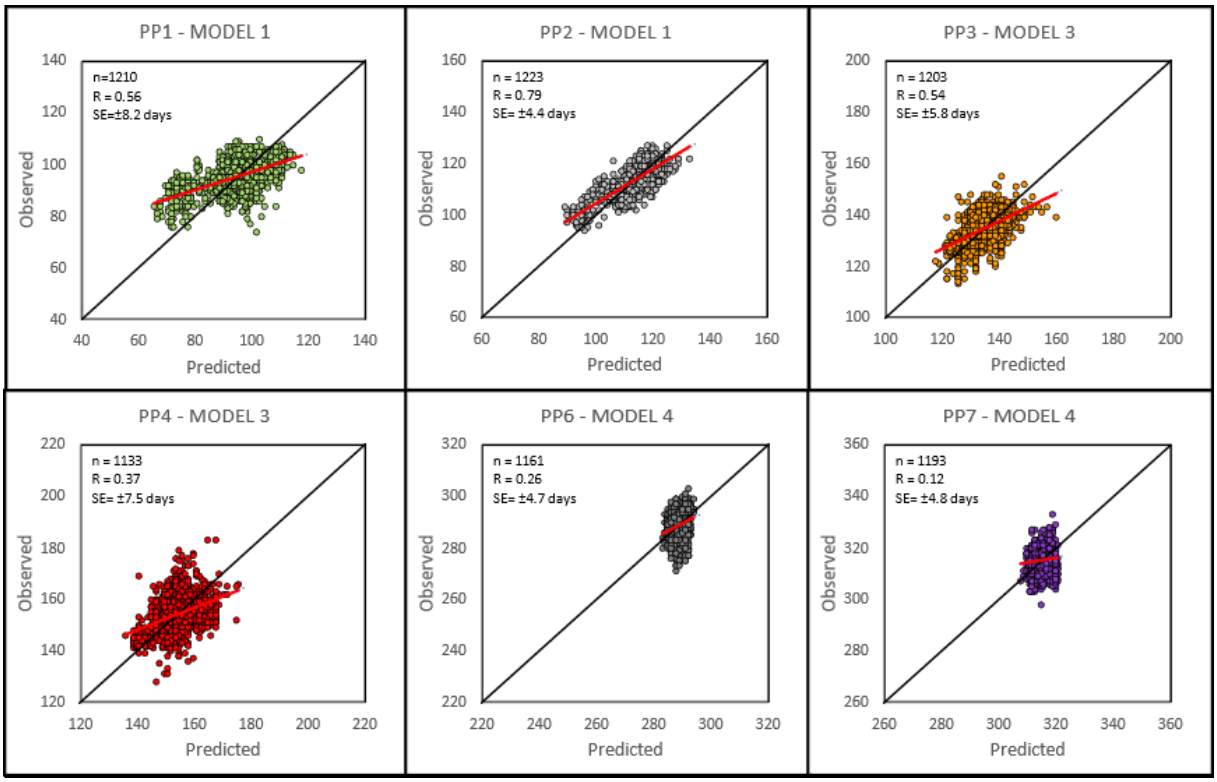

Figure 4: Statistics of the best choosen phenological models of oak for prediction of spring (PP1-PP4) and autumn (PP6-PP7) phenological phases (MODEL 1 – Spring warming, MODEL 3 – Spring photo-chilling, MODEL 4 – Autumn cooling-shortening)

Discussion

The results of our study are generally corresponding to the findings reported by BASLER et al. (2016), that the lowest average prediction errors for spring phenology (leaf unfolding) ranged from ±7 to ±9 days for the dataset pooled across sites and years. Only in the case of beech and the phenological phase PP1, the upper limit was exceeded in our study. On the contrary, the prediction error for oak was lower than 7 days for two of four spring phenological phases.

Inclusion of daylength and chilling requirements (MODEL 2 and 3) improved predictions of spring phenological phases for beech forest stands comparing to warming model (MODEL 1). Warming model brings comparable results with more complex photo-chilling model for prediction of PP1 and PP2 in oak forest stands. The stated results correspond to the knowledge of DANTEC et al.(2014), that Sessile oak (*Quercus petraea* (MATT.) LIEBL.) has relatively low chilling requirements, although it has higher heat requirements compared to species such as European Beech (*Fagus sylvatica* L.) and contrary, beech is well-known by high chilling requirements.

Autumnal model (MODEL 4) is less sensitive as spring models and its precision is similar or higher. The autumn phenology prediction error did not exceed two-thirds of the error reported in LIU et al. (2020), where the same type of model was applied, but the phenological observations were ground-based and captured a wider latitudinal gradient (entire area of Germany). Therefore, our plan is to verify the accuracy of the model for different latitudes of the temperate zone or reparametrize the model on data from a wider latitudinal gradient. The motivation arises from our findings that the use of different sets of parameters brought relatively significant differences in the results of modelling autumn phenological phases (PP6-PP7), and in this direction we are open to a new cooperation. Another challenge is

a more complex validation of phenological models on production processes after their planned connection with the Sibyla Lex Eterna process-based model, which is being developed at the Technical University in Zvolen.

Acknowledgment

The study was supported by the Slovak Research and Development Agency under the contracts No. APVV-19-0035.

Literature

BASLER, D. (2016): Evaluating phenological models for the prediction of leaf-out dates in six temperate tree species across central Europe. Agricultural and Forest Meteorology 217: 10–21. https://doi.org/10.1016/j.agrformet.2015.11.007

CAFFARRA, A.; DONNELLY, A.; CHUINE, I. (2011): Modelling the timing of Betula pubescens budburst. II. Integrating complex effects of photoperiod into process-based models. Climate Research 46(2): 159–170. https://doi.org/10.3354/cr00983

CORNES, R.C.; VAN DER SCHRIER, G.; VAN DEN BESSELAAR, E.J.M.; JONES, P.D. (2018): An Ensemble Version of the E-OBS Temperature and Precipitation Data Sets. Journal of Geophysical Research: Atmospheres 123(17): 9391–9409. https://doi.org/10.1029/2017JD028200

DANTEC, C.F.; VITASSE, Y.; BONHOMME, M.; LOUVET, J.-M.; KREMER, A.; DELZON, S. (2014): Chilling and heat requirements for leaf unfolding in European beech and sessile oak populations at the southern limit of their distribution range. International Journal of Biometeorology 58(9): 1853–1864. https://doi.org/10.1007/s00484-014-0787-7

DELPIERRE, N.; DUFRÊNE, E.; SOUDANI, K.; ULRICH, E.; CECCHINI, S.; BOÉ, J.; FRANÇOIS, C. (2009): Modelling interannual and spatial variability of leaf senescence for three deciduous tree species in France. Agricultural and Forest Meteorology 149(6): 938–948. https://doi.org/10.1016/j.agrformet.2008.11.014

FABRIKA, M.; PRETZSCH, H. (2013): Forest ecosystem analysis and modelling, 1. ed. Zvolen, Technical University. 620 S.

FADDEN, D. (2019): Phenological characteristics of Sitka spruce, oak and beech growing in Ireland [MSc Thesis]. University College Dublin. 89 S.

FU, Y.; ZHANG, H.; DONG, W.; YUAN, W. (2014): Comparison of Phenology Models for Predicting the Onset of Growing Season over the Northern Hemisphere. PLOS ONE 9(10): e109544. https://doi.org/10.1371/journal.pone.0109544

GARONNA, I.; DE JONG, R.; DE WIT, A.J.W.; MÜCHER, C.A.; SCHMID, B.; SCHAEPMAN, M.E. (2014): Strong contribution of autumn phenology to changes in satellite-derived growing season length estimates across Europe (1982–2011). Global Change Biology 20(11): 3457–3470. https://doi.org/10.1111/gcb.12625

GRAY, J.; SULLA-MENASHE, D.; FRIEDL, M.A. (2019): User Guide to Collection 6 MODIS Land Cover Dynamics (MCD12Q2) Product

HÄNNINEN, H. (1990): Modelling bud dormancy release in trees from cool and temperate regions. Silva Fennica 0(213).

KEENAN, T.F.; GRAY, J.; FRIEDL, M.A.; TOOMEY, M.; BOHRER, G.; HOLLINGER, D.Y.; MUNGER, J.W.; O'KEEFE, J.; SCHMID, H.P.; WING, I.S.; YANG, B.; RICHARDSON, A.D. (2014): Net carbon uptake has increased through warming-induced changes in temperate forest phenology. Nature Climate Change 4(7): 598–604. https://doi.org/10.1038/nclimate2253

KLOSTERMAN, S.T.; HUFKENS, K.; GRAY, J.M.; MELAAS, E.; SONNENTAG, O.; LAVINE, I.; MITCHELL, L.; NORMAN, R.; FRIEDL, M.A.; RICHARDSON, A.D. (2014): Evaluating remote sensing of deciduous forest phenology at multiple spatial scales using PhenoCam imagery. Biogeosciences 11(16): 4305–4320. https://doi.org/10.5194/bg-11-4305-2014

LIU, Q.; PIAO, S.; CAMPIOLI, M.; GAO, M.; FU, Y.H.; WANG, K.; HE, Y.; LI, X.; JANSSENS, I.A. (2020): Modeling leaf senescence of deciduous tree species in Europe. Global Change Biology 26(7): 4104–4118. https://doi.org/10.1111/gcb.15132

MELAAS, E.K.; FRIEDL, M.A.; RICHARDSON, A.D. (2016): Multiscale modeling of spring phenology across Deciduous Forests in the Eastern United States. Global Change Biology 22(2): 792–805. https://doi.org/10.1111/gcb.13122

MELAAS, E.K.; RICHARDSON, A.D.; FRIEDL, M.A.; DRAGONI, D.; GOUGH, C.M.; HERBST, M.; MONTAGNANI, L.; MOORS, E. (2013): Using FLUXNET data to improve models of springtime vegetation activity onset in forest ecosystems. Agricultural and Forest Meteorology 171–172: 46–56. https://doi.org/10.1016/j.agrformet.2012.11.018

MENG, L.; ZHOU, Y.; GU, L.; RICHARDSON, A.D.; PEÑUELAS, J.; FU, Y.; WANG, Y.; ASRAR, G.R.; DE BOECK, H.J.; MAO, J.; ZHANG, Y.; WANG, Z. (2021): Photoperiod decelerates the advance of spring phenology of six deciduous tree species under climate warming. Global Change Biology 27(12): 2914–2927. https://doi.org/10.1111/gcb.15575

PEANO, D.; MATERIA, S.; COLLALTI, A.; ALESSANDRI, A.; ANAV, A.; BOMBELLI, A.; GUALDI, S. (2019): Global Variability of Simulated and Observed Vegetation Growing Season. Journal of Geophysical Research: Biogeosciences 124(11): 3569–3587. https://doi.org/10.1029/2018JG004881

PIAO, S.; WANG, X.; PARK, T.; CHEN, C.; LIAN, X.; HE, Y.; BJERKE, J.W.; CHEN, A.; CIAIS, P.; TØMMERVIK, H.; NEMANI, R.R.; MYNENI, R.B. (2020): Characteristics, drivers and feedbacks of global greening. Nature Reviews Earth & Environment 1(1): 14–27. https://doi.org/10.1038/s43017-019-0001-x

RICHARDSON, A.D.; KEENAN, T.F.; MIGLIAVACCA, M.; RYU, Y.; SONNENTAG, O.; TOOMEY, M. (2013): Climate change, phenology, and phenological control of vegetation feedbacks to the climate system. Agricultural and Forest Meteorology 169: 156–173. https://doi.org/10.1016/j.agrformet.2012.09.012

SARVAS, R. (1974): Investigations on the annual cycle of development of forest trees, Autumn dormancy and winter dormancy. Communicationes Instituti Forestalis Fenniae 84: 1–101.

STÖCKLI, R.; RUTISHAUSER, T.; BAKER, I.; LINIGER, M.A.; DENNING, A.S. (2011): A global reanalysis of vegetation phenology. Journal of Geophysical Research: Biogeosciences 116(G3). https://doi.org/10.1029/2010JG001545

WAREING, P.F. (1953): Growth Studies in Woody Species V. Photoperiodism in Dormant Buds of Fagus sylvatica L. Physiologia Plantarum 6(4): 692–706. https://doi.org/10.1111/j.1399-3054.1953.tb08442.x

WHITE, M.A.; THORNTON, P.E.; RUNNING, S.W. (1997): A continental phenology model for monitoring vegetation responses to interannual climatic variability. Global Biogeochemical Cycles 11(2): 217–234. https://doi.org/10.1029/97GB00330